

Green Synthesis, Characterization and Electrical Properties of Iron Doped Vanadium Oxide for Strain Gauges

T. R. Kishan Chand¹, H. M. Kalpana^{1*} and H. S. Lalithamba²

¹Department of Electronics and Instrumentation Engineering, Siddaganga Institute of Technology, Tumakuru-572103, Karnataka, India. *e-mail address: kalpanahm@sit.ac.in

²Department of Chemistry, Siddaganga Institute of Technology, Tumakuru-572103, Karnataka, India.

Abstract

A series of vanadium oxide (V_2O_5) nanoparticles containing small varying concentrations of iron (Fe) were synthesized using green protocol to test its suitability towards strain gauges. The morphological, structural, transmission spectral and the dielectric properties of the synthesized nanoparticles were characterized using SEM, HRTEM, XRD, FTIR and the LCR meter respectively. The structural analysis results depict a transformation from amorphous to orthorhombic cubic phased crystalline structure. The morphological data denote an improvement in the appearance of the samples without any cracks. A better electronic transition due to high activation energy was observed from the slight shift of the transmission spectral peaks towards the lower wave number. The improved conductivity from 5.37 to 12.51 S/m in conjunction with the better temperature characteristics, specially incase of 15 wt% Fe:V₂O₅ contributes to the enhanced sensitivity of the samples. The overall results from the characterization emphasize the synthesized nanoparticle's remarkable attributes towards the fabrication of thin film strain gauges.

Keywords: Nanoparticles, vanadium oxide, iron, electrical properties, strain gauge

1.0 Introduction

In the present scenario, thin film strain gauges are considered as a better possibility for many practical applications in comparison with unbonded, bonded, metallic and foil type strain gauges [1]. Strain gauges are the material whose resistance is responsive to strain [2]. Despite their inability to tolerate changes in air temperatures that affect their normal operation, they can be designed and constructed in such a way that their inconsistencies are cancelled out. This can be accomplished by choosing a material that has corrosion resistance, strong electrochemical performance, good temperature coefficient of resistance and low thermal coefficient of expansion [3]. The usage of dopants during synthesis helps in

addressing several of the disadvantages associated with the materials for strain gauges. It also assists in the reduction of transitioning temperatures by strengthening the thermoelectric characteristics [4]. Considering this, vanadium oxide has been systematically synthesized with the varying concentrations of iron as dopant. In this procedure the Butea Monosperma Seeds (BMS) is utilized as the fuel to serve the purpose of green protocol in generating the doped samples. The seeds can be obtained from many parts of the tropical region of Indian subcontinent. They are popularly known as the flame of forest in palashi of West Bengal.

Vanadium is a reliable material and has a leap across the research spectrum because of its simplicity in synthesis, excellent safety profile qualities, large

specific capacity along with the energy density [5]. Its huge availability of resources at very minimal price has also assisted in serving the purpose [6, 7]. A variety of forms is being exhibited by the vanadium in its oxide family that includes V_2O_3 , V_2O_4 , V_2O_5 , V_3O_5 , V_4O_7 , V_5O_9 , V_6O_{11} , V_6O_{18} and V_7O_{18} . Due to its stability, vanadium in its pentoxide (V_2O_5) form is gaining a substantial edge over its other variants [8]. It narrows band gap, making it an ideal material for photonics, rechargeable has a propensity for exhibiting an excellent metal to semiconductor transition by assuming a rapid shift in its electrical properties [9]. The material can widely be noticed across the healthcare, automobile, smart windowing, water electrolysis, UV sensors, ultra capacitors, high temperature semiconductors, thermo-chemical sensing and structural applications according to the investigation [10]. The V_2O_5 nanomaterial exhibits three distinct phases that includes α , β and γ , out of which the α phase exhibits greater stability and a batteries, electrolytic and sensor-related applications [11]. The electrical characteristics of nanostructured V_2O_5 are superior to that of their bulk counterparts due to the obvious increased surface area generated by its superfine particle size [12].

Alloys, metals, semiconductors and polymers are among the materials frequently used in strain gauge applications [13]. The present work, which is on the doped synthesis of an inorganic compound-based nanocrystal, is a fresh take considering the recent trends. It is known that an interaction between vanadium oxides and dopants will have an impinging impact on the dielectric behavior of the samples. Many researchers are interested in studying its suitability for a range of applications, such as microwave devices and solar energy control of buildings, due to the abrupt change in its opto-electrical and structural features observed on the addition of dopant. Also there are very minimal studies being conducted on these samples for their feasibility towards strain gauge application. This work provides an exclusive assessment on the electrical properties of Fe: V_2O_5 and its suitability with strain gauges.

Nanocrystalline materials are the optimum choice for any strain gauge application due to its smaller grain size, increase in grain boundary density, enhanced sensitivity, and limited performance deterioration [14]. The selectivity of sensors is highly dependent on particle size, time, internal porosity and surface shape [15]. Spray drying, nanostructural assembling, sol-gel, microwave irradiation, hydrothermal and combustion synthesis are some of the approaches to integrate dopants into the V_2O_5

structure [16, 17]. Each of these approaches has its own set of constraints and merits, but current investigation prefers the combustion synthesis as it creates nanoparticles with excellent chemical purity [18]. Nanobelts, nanosheets, nanorods, nanotubes and nanoneedles are some of the forms in which the materials evolve out of combustion synthesis [19]. Any shape that lies within the nanometer scale range will help in assisting the strain gauges to perform better.

Iron (Fe), an element which is found in abundance at the inner as well as the outer area of the earth's crust is commonly found in two oxidation states of iron (II) and iron (III). Recently it is observed in most of the medical, industrial and research oriented applications [20]. The material is also seeking greater attention amongst the researchers because of its easier separation techniques, good surface-volume ratio, super-paramagnetic ability, better surface area, chemical efficiency and inexpensiveness [21]. Recently the usage of iron as a dopant into a transition metal has been investigated for the application of spintronic and magnetic recording devices [22]. By taking these literatural outcomes, the material is used as a dopant with varying concentrations of 5, 10, 15 wt%. The material when dissolved with the assistance of nitric acid forms a yellow solution due to hydrolysis and when heated, the nitric acid gets evaporated by precipitating all the iron into the precursor sample during combustion.

2.0 Experimentation

In order to generate the 5, 10, and 15 wt% concentration of Fe: V_2O_5 nanoparticles, a quantum of 0.604, 1.209 and 1.813g of ferric nitrate $Fe(NO_3)_3$ dopants are added to an equivalent quantity of 5.556, 5.264 and 4.971g of ammonium metavanadate (NH_4VO_3) precursor. Then 60 ml of deionized water is utilized to dissolve the measured samples along with few drops of nitric acid. The solution containing the mixture is then sonicated for an hour, until the samples are thoroughly homogenized. These are heated to 500°C inside the muffle furnace. After an hour, the V_2O_5 is observed to change into a diminished Fe: V_2O_5 in the form of a foamy extract, which is then calcinated to collect the fine Fe: V_2O_5 nanoparticles.

The CLR meter was used to evaluate dielectric properties such as conductivity and impedance of the synthesized material at various temperatures. A hydraulic press was used to construct pellets composed of nanoparticles with a diameter of 10 mm

and a thickness of 1-3 mm for this purpose. A spring-loaded holder is then preferred to sandwich the pellets between the two brass electrodes. Finally, the entire assembly is placed inside the furnace monitored by temperature controller, for the investigation of its variation in dielectric properties with temperature.

2.1 Characterization Techniques

In this research work, XRD was used to examine the structural characteristics of the Fe: V₂O₅ (Model: Rigaku smart lab, Japan). SEM (Model: ESEM Quanta 200) and HRTEM (Model: FEI Titan 80-300) were used to conduct morphological analyses. EDX is used to determine the elemental makeup of these samples (Model: Ohring 1992). The FTIR is used for transmission spectral analysis to examine functional groups and chemical bonding structure (Model: Bruker alpha, wavelength range: 600 to 1500 cm⁻¹). Using a CLR meter (Model: HIOKI-IM3536), probes (Model: HIOKIL-2000), and a temperature controller (Model: DPI-120), the dielectric characteristics of the pellet samples were measured.

3.0 Results and Discussions

As previously stated, the produced Fe:V₂O₅ nanoparticles are submitted to several characterization techniques in order to determine their appropriateness towards strain gauges. The effects of frequency and temperature changes on its AC conductivity are closely examined, and the results are explained briefly in the coming section.

3.1 Structural Analysis

The X-Ray diffractometer (XRD) was used to investigate the structural analysis of synthesized doped and undoped nanoparticles using the Cu-K α radiation at $\lambda = 1.54 \text{ \AA}$ and a bragg's angle of 10-90° as an x-ray source. The results are shown in Fig.1. The crystal planes found are indexed to V₂O₅ orthogonal phased cubic crystal structure (JCPDS 41-1426), which is confirmed by the characteristic peak of diffraction found at $2\theta = 26.18^\circ$ corresponding to (101). The crystalline structure of the nanoparticles is depicted by the prominent peak at $2\theta = 31.06^\circ$ and orientation of (110) at the center. The extent of crystallization relies on the weight percentages of dopant incorporated. The absence of any detectable organic contaminants in conjunction with the vanadium oxide can be seen from the short narrow peaks around it.

Fig.1. also shows a modest shift in the peak towards lower angle, which can be attributed to raise in atomic

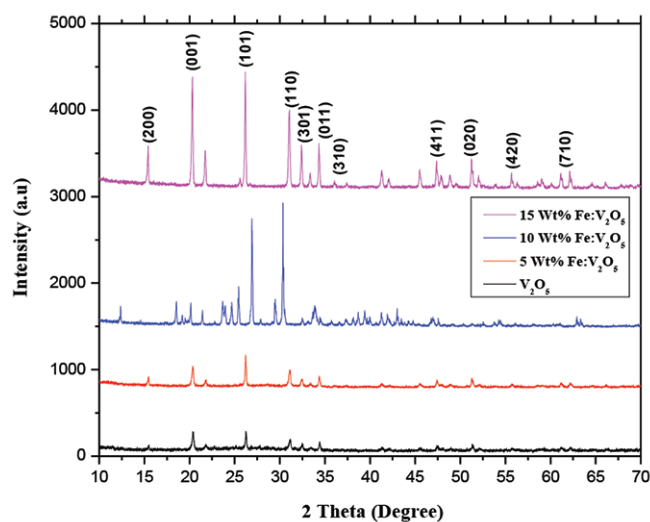


Figure 1: XRD results of the synthesized Fe:V₂O₅ nanoparticles

layer distance and decreased interlayer spacing of the doped vanadium samples. As the dopant concentration increases, the strength of the peak follows up the same, along with the width in the planes of diffraction broadening up. The average crystallite size, micro strain, and dislocation density of the nanoparticles determined using scherrer's theory were 5.6336 \AA , 0.06426×10^{-3} , and $0.0315 \times 10^{16}/\text{m}^2$, which results in contributing to the better sensitivity and conductivity of strain gauges [23].

3.2 Morphological Studies

In this study, scanning electron microscopic (SEM) pictures are used to examine the micro structural features of the nanoparticles. The thin rod shaped structure with a uniform surface and smooth edges in the size range of 1-10 nm is clearly seen from the photographs presented in Fig.2. Despite the fact that the shape of 5 wt% Fe:V₂O₅ nanorods does not differ significantly from that of pure once, a good homogeneous porosity without any cracks can be recognized, as the wt% concentration of dopant increases. It's also worth mentioning that the morphology shifts from amorphous to crystalline phase structure with minimal atomic displacement. This suggests that by composing a vast number of small units of cohesive morphological structure, the samples have an improved structural appearance and stability.

Due to the rhombohedra motif structure noticed after adding dopants, some areas of the image are considerably deformed and distorted. The reorientation in lattice structure with an improved

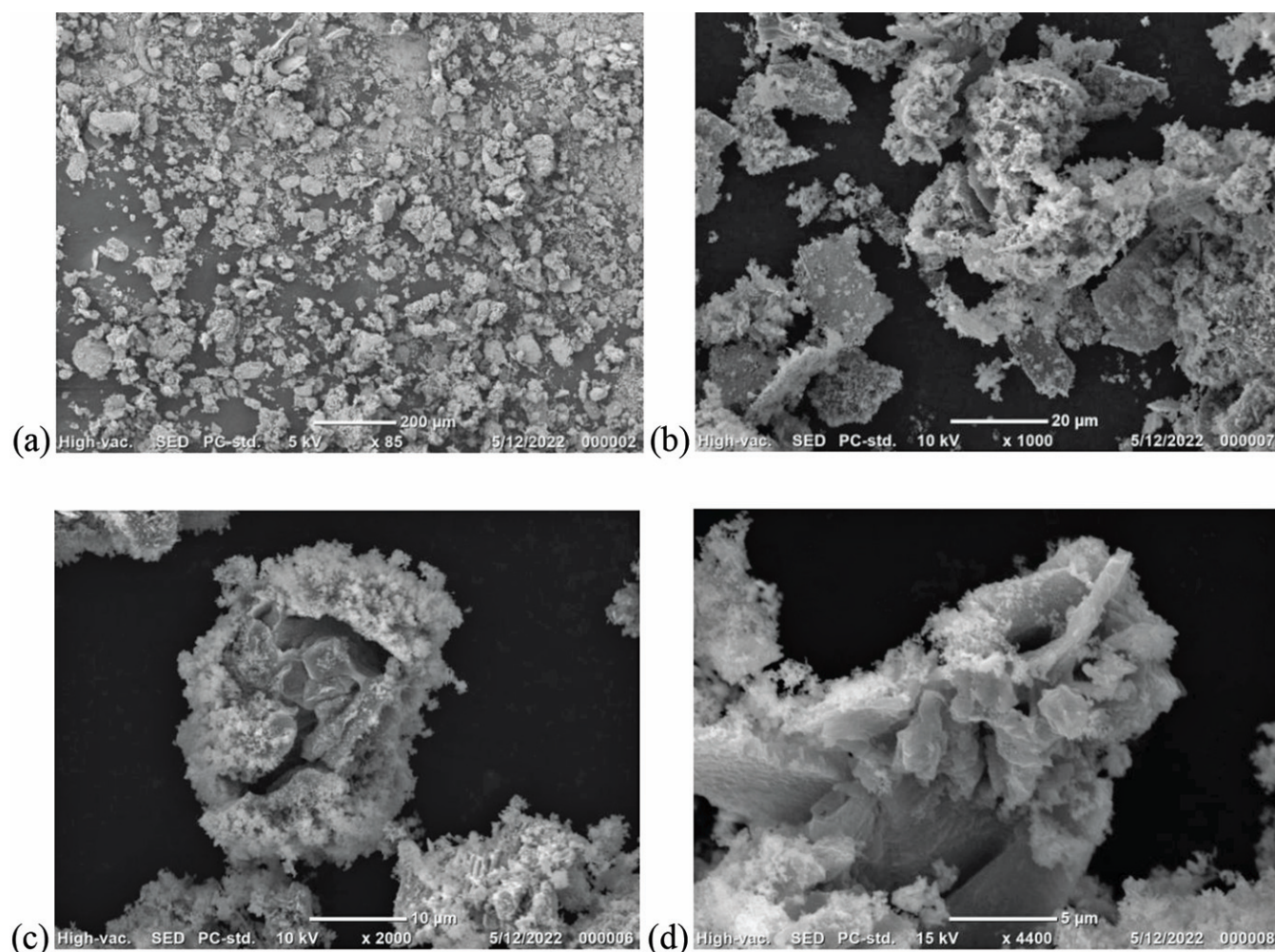


Figure 2: SEM images of synthesized $\text{Fe}:\text{V}_2\text{O}_5$ nanoparticles (a) Pure, (b) 5 wt% $\text{Fe}:\text{V}_2\text{O}_5$, (c) 10 wt% $\text{Fe}:\text{V}_2\text{O}_5$, (d) 15 wt% $\text{Fe}:\text{V}_2\text{O}_5$

cyclic stability can be observed with the raise in dopant concentration. Another interesting finding is that, the inclusion of dopant has no effect on the formation of crystalline phase even at different concentrations.

Fig.3. shows the high resolution images of the synthesized nanoparticles (HRTEM). The strong vanadyl bonding structure is represented by the sheet-shaped image with the black dots. The Fig.3(c). shows the lattice planes with an inter-planar distance (d-space) of ~ 0.6 nm (corresponding to 101 planes) in 2 to 5 nm size range. This signifies that the nanoparticles have a considerable crystallite size, which adds to the enhanced quality of strain gauges. The dopants are commonly located at the subsurface, surface periphery or scattered around the vanadium oxides uniformly.

3.4 Transmission Spectral Analysis

Transmission spectroscopy in between the range of $600\text{-}1500$ cm^{-1} wave number was used to investigate the functional groups and chemical bonds of synthesized nanoparticles. The FTIR spectrum of doped sample shows three distinct vibration modes around 833.13 , 1018.63 and 1370.04 cm^{-1} , as can be visible from the schematic. The peak observed at 1018.63 cm^{-1} is caused by $\text{V}=\text{O}$ symmetric stretching, which shifts towards the lower wave number as the dopants are introduced. This could be linked to the interaction of them with the vanadyl bonding structure, which has resulted in increment in the crystallite size of nanoparticles. The asymmetric stretching band at 833.13 cm^{-1} is related to the reduction of valence state observed on the electron moving from V^{5+} to V^{4+} of the V_2O_5 crystals, while the symmetric stretching

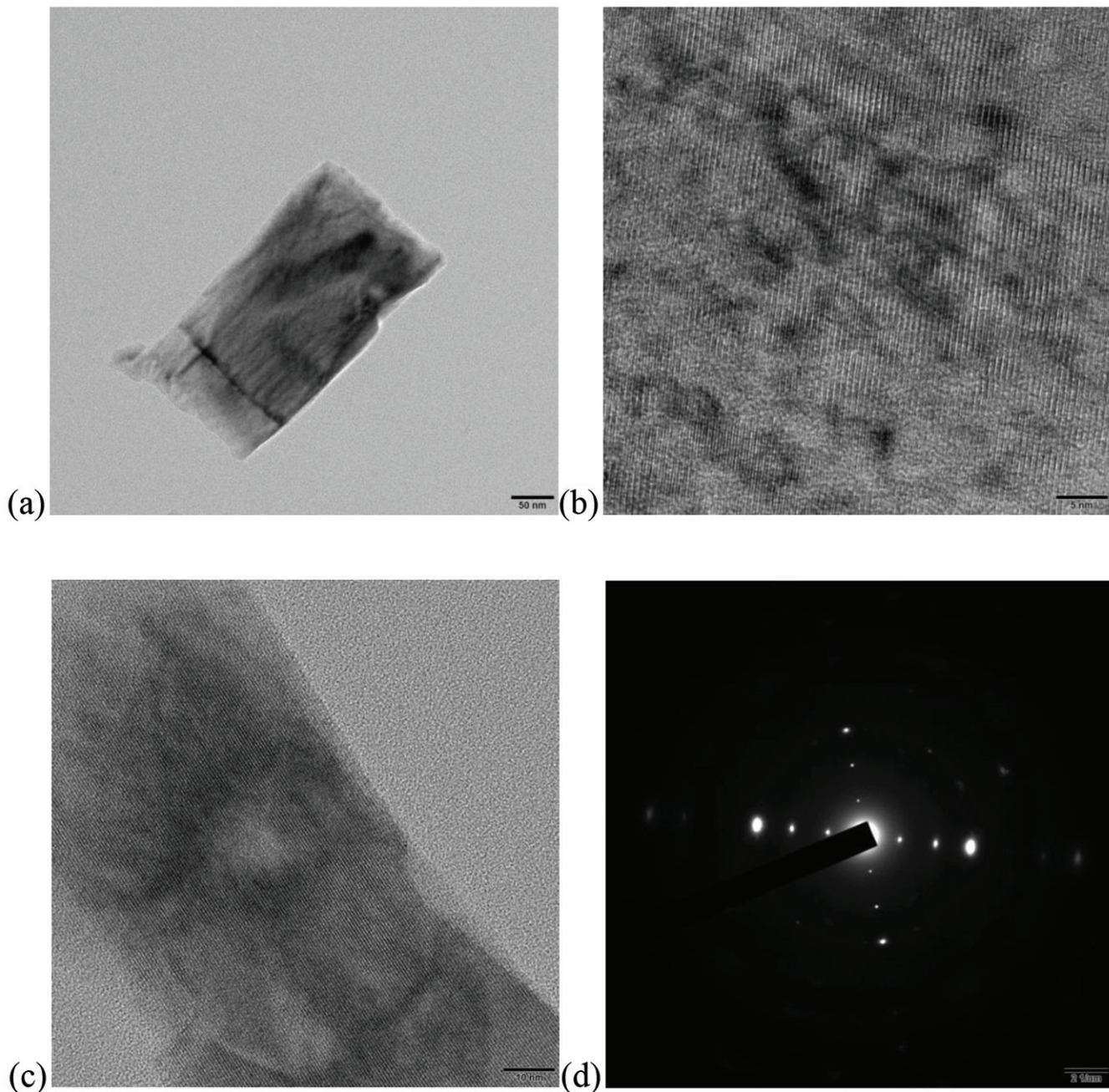


Figure 3: (a), (b), (c) HRTEM images of synthesized Fe:V₂O₅ nanoparticles, (d) SAED pattern of Fe:V₂O₅ nanoparticles

band at 1370.04 cm⁻¹ corresponds to orthogonal crystalline structure.

4.0 Dielectric Properties

Analysis of dielectric properties is essential for any strain gauge application because they provide

significant details about the synthesized material such as, activation energy, conductivity, impedance and dielectric loss. The microstructures, crystal orientation and stoichiometry of V₂O₅ nanoparticles influence their dielectric characteristics. As a consequence, a thorough examination report obtained from the CLR meter, conducted for varied frequency and temperatures is evaluated and discussed.

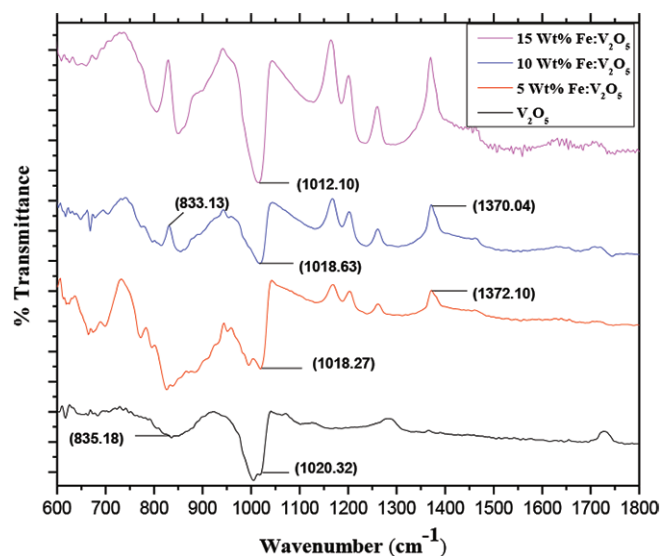


Figure 5: FTIR spectrum of synthesized Fe:V₂O₅ nanoparticles

4.2 Conductivity

From the literatural references, it can be noticed that the existence of electron free carriers, material composition, temperature and the method of synthesis greatly influences the conductivity of any material. The addition of dopant serves in generating free charge carriers [24]. Due to the introduction of an electric field, the conductivity of samples can either raise or reduce, according to the nature of dopant. As can be seen from the Fig.6, the conductivity of V₂O₅ varies from 5.37 to 12.51 S/m with the varying dopant concentration, which can be attributed to hopping of electrons from V⁴⁺ to V⁵⁺ ions, occurring in-between the space of vanadium atoms which are placed in a differently charged state.

4.2 Analysis of Conductivity with Frequency at Varied Concentrations of Dopant

Fig.6. shows the influence of conductivity on frequency for varying dopant concentrations of Fe:V₂O₅ nanoparticles. The conductivity is virtually frequency independent at lower range, but as the frequency rises, a larger dependency appears. The low frequency at which the conductivity is independent of the effect causing it is regarded as the DC conductivity region. The conduction mechanism found due to electron translational hopping is responsible for the observed linearity of conductivity response with frequency in the middle. Due to better localized electron hopping and series resistance effects, the third

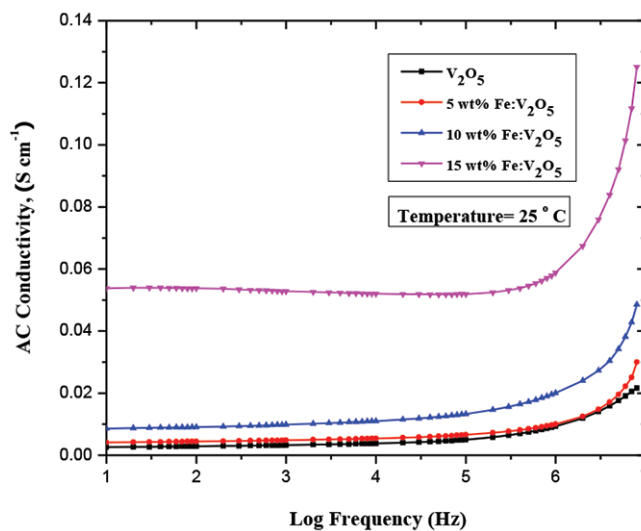


Figure 6: Variation of AC conductivity with frequency of the V₂O₅ and Fe:V₂O₅

group in the end displays a tiny exponential raise in conductivity with frequency. Because of the increased charge carriers within the material, there is an improvement in the amplitude of variation in conductivity with change in frequency. The maximum conductivity of the nanoparticles is obtained for 15 wt% Fe:V₂O₅ samples, as can be seen from the graphical plots.

This is due to enormous number of charge carriers with greater activation energy, which boosts the electron mobility and causes them to drift at a faster rate towards the electrodes. Any increase of dopants beyond this threshold causes the crystallite size of the samples to expand, impeding the passage of free electronic carriers and thereby resulting in a loss in conductivity.

4.3 Analysis of Impedance with Frequency at Varied Concentrations of Dopant

The combined effects of ohmic resistance and reactance produce impedance, often known as the effective resistance offered by an electric circuit to alternating current. Because of the charge carrier resistance, if at any time the frequency of electric field is low, the free electron carriers are forced to flow across a long distance, resulting in lower conductivity. When the frequency of the applied field rises, the case reverses with a compressed mean displacement path, which is demonstrated in the Fig.7.

The results from the CLR meter shows that among the many variations of the produced nanoparticles,

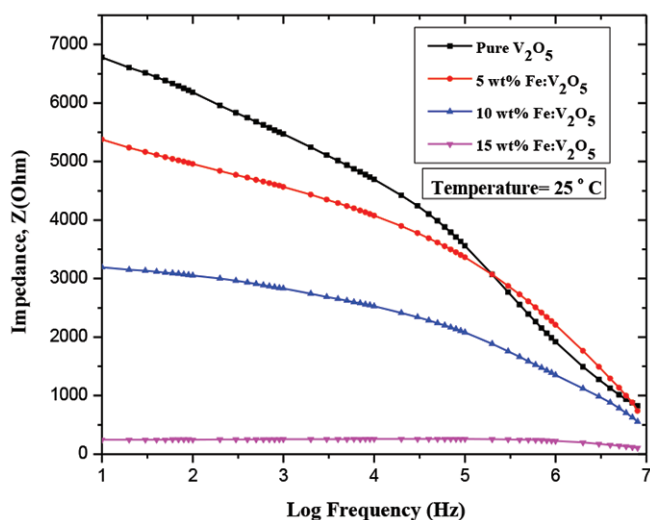


Figure 7: Variation of impedance with log frequency of V_2O_5 and $Fe:V_2O_5$

the 15 wt% $Fe:V_2O_5$ exhibits stronger dielectric characteristics than its counterparts. Any increase in the concentration of dopant beyond 15 wt%, in order to evaluate its acceptable properties will result in the deterioration of vanadium oxide's distinctive attributes. Hence the 15 wt% $Fe:V_2O_5$ samples are used as a reference for further research into their appropriateness towards strain gauges.

4.4 Analysis of Conductivity and Impedance with Temperature amongst 15 wt% $Fe:V_2O_5$ Samples

The conductivity and impedance of $Fe:V_2O_5$ samples containing 15 wt% concentration are investigated at various temperatures. These findings are then displayed in the Fig.8 and Fig.9. The conductivity and impedance of nanoparticles may raise or lapse with temperature, based on the type of dopant used during synthesis.

The higher molecular conduction observed due to the progressive increase in temperature is considered as the cause for the increase in conductivity and decrease in impedance, recorded in this study. This might also be related to the increased magnitude of free charge carriers generated by the interlayer spacing of synthesized nanoparticles. The earlier increase in conductivity could be attributed to the adsorption being observed due to the presence of water molecules, which would gradually vanish as the temperature rises. The AC conductivity in particular is the sum total of DC conductivity caused by free charge movement and the polarization

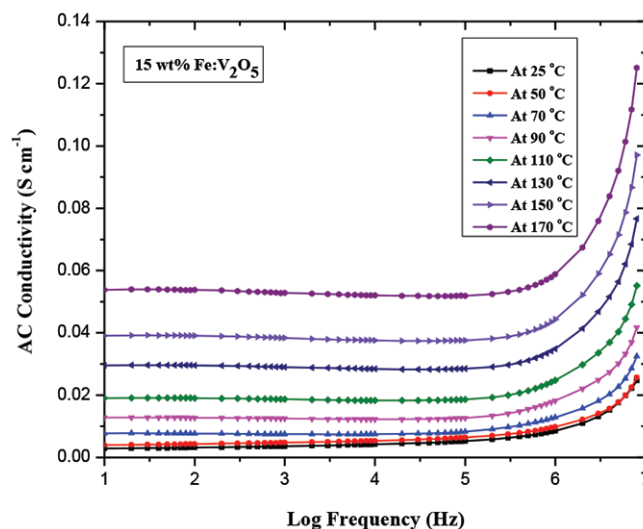


Figure 8: Variation of AC conductivity with Log frequency of 15 wt% $Fe:V_2O_5$

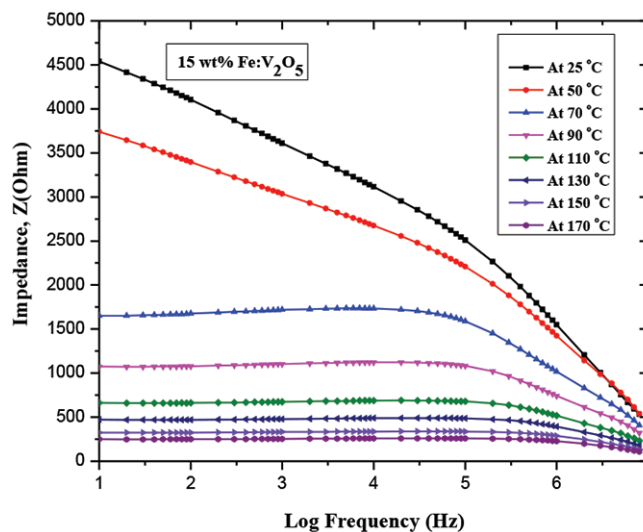


Figure 9: Variation of Impedance with Log frequency of 15 wt% $Fe:V_2O_5$

conductivity caused by bound charge movement. Any increase in temperature causes the composite DC conductivity to increase, competing with the polarization conductivity, resulting in a shift in overall response of samples. As the temperature rises further, the transition point from the independent to dependent zone begins to shift towards the higher frequency range. If the temperature is kept constant at this stage, the charge carrier's relaxation time becomes minimal, resulting in an overall increase in material's conductivity.

5.0 Conclusions

The nano-structured samples in this study, due of its ultrafine diameter have better electrical properties than that of its bulker counterparts. Due to the enhancement of conductivity from 5.37 to 12.51 S/m (specially in the case of 15 wt% Fe:V₂O₅), it can be inferred that these synthesized samples are successful in providing a favorable outcome for the application of strain gauges. The raise in surface charges and interfacial polarization caused by the addition of dopant are related to the improvement in overall dielectric characteristics. Hence from these results, it can be concluded that the addition of dopant to an oxide sample helps to stabilize the nanoparticle structure and leads in bringing up positive changes in shape, sensitivity and responsiveness in its electrical characteristics.

Acknowledgements

The authors are grateful to, "Siddaganga institute of technology", Tumakuru-572103, Karnataka, India for supporting this research work.

References

1. Zhao, Yinming, Yang Liu, Yongqian Li, and Qun Hao. (2020): "Development and application of resistance strain force sensors." *Sensors*, 20, no. 20, p.5826.
2. O.O. Oluwole, A. T. Olanipekun, and O.O. Ajide. (2015): "Design, construction and Testing of a strain gauge Instrument." *Int. J. Sci. Eng. Res*, 6, pp. 1825-1829.
3. Tutak, Piotr. (2014): "Application of strain gauges in measurements of strain distribution in complex objects." *Journal of Applied Computer Science Methods*, 6.
4. Carofiglio, Marco, Sugata Barui, Valentina Cauda, and Marco Laurenti. (2020): "Doped zinc oxide nanoparticles: synthesis, characterization and potential use in nanomedicine." *Applied Sciences*, 10, no. 15, p. 5194.
5. Liang Xing, Guohua Gao, Yindan Liu, Tianqi Zhang, and Guangming Wu. (2017): "Synthesis and characterization of Fe-doped vanadium oxide nanorods and their electrochemical performance." *Journal of Alloys and Compounds*, 715.
6. Zhang, Yanqing, Weiming Xiong, Weijin Chen, and Yue Zheng. (2021): "Recent progress on vanadium dioxide nanostructures and devices: fabrication, properties, applications and perspectives." *Nanomaterials*, 11, no.2, p.338.
7. Li Yanwei, Jinhuan Yao, Evan Uchaker, Ming Zhang, Jianjun Tian, Xiaoyan Liu, and Guozhong Cao. (2013): "Sn-doped V₂O₅ film with enhanced lithium-ion storage performance." *The Journal of Physical Chemistry C*, 117, 45, pp.23507-23514.
8. A Salimian, S. Ketabi, and H. R. Aghabozorg. (2018): "Hydrogen storage comparison of M doped vanadium oxide nanotubes (M=Mo, Zr and W): A molecular simulation study." *International Journal of Hydrogen Energy*, 43, no. 5, pp. 2831-2839.
9. M. Farahmandjou, and N. Abaeiyan. (2017): "Chemical synthesis of vanadium oxide V₂O₅ nanoparticles prepared by sodium metavanadate." *Journal of Nanomedicine Research*, 5, no. 1.
10. Kianfar, Ehsan. (2019): "Recent advances in synthesis, properties, and applications of vanadium oxide nanotube." *Microchemical Journal*, 145, pp. 966-978.
11. Venkatesan, Arumugam, Nagamuthu Raja Krishna Chandar, Arumugam Kandasamy, Madhu Karl Chinnu, Kalusalingam Nagappan Marimuthu, Rangasamy Mohan Kumar, and Ramasamy Jayavel. (2015): "Luminescence and electrochemical properties of rare earth (Gd, Nd) doped V₂O₅ nanostructures synthesized by a non-aqueous sol-gel route." *RSC Advances*, 5, no. 28, pp. 21778-21785.
12. Zhou, Xiao-xia, Jing-fu Liu, and Gui-bin Jiang. (2017): "Elemental mass size distribution for characterization, quantification and identification of trace nanoparticles in serum and environmental waters." *Environmental Science & Technology*, 51, no. 7, pp. 3892-3901.
13. Gnanasambanthan, Harish, Sharmila Nageswaran, and Debashis Maji. (2019): "Fabrication of Flexible Thin Film Strain Sensors using Kapton Tape as Stencil Mask." *International Conference on Vision towards Emerging Trends in Communication and Networking (ViTECoN)*, IEEE, pp. 1-4.
14. Rida A, Micoulaut M, Rouhaud E, & Makke, A. (2020): "Understanding the strain rate sensitivity of nanocrystalline copper using molecular dynamics simulations." *Computational Materials Science*, 172, p. 109294.

15. Alghool, Samir, Hanan F. Abd El- Halim, and Ayman M. Mostafa. (2019): "An eco-friendly synthesis of V₂O₅ nanoparticles and their catalytic activity for the degradation of 4-nitrophenol." *Journal of Inorganic and Organometallic Polymers and Materials*, 29, no. 4, pp. 1324-1330.
16. Ealia S and M. P. Saravanakumar. (2017): "A review on the classification, characterisation, synthesis of nanoparticles and their application." In IOP Conference Series: Materials Science and Engineering, 263, no. 3, p. 032019.
17. A. Jagadeesh, T. Mimani Rattan, M. Muralikrishna, and K. Venkataramaniah. (2014): "Instant one step synthesis of crystalline nano V₂O₅ by solution combustion method showing enhanced negative temperature coefficient of resistance." *Materials Letters*, 121, pp. 133-136.
18. Chaitra. C, H. M. Kalpana, C. M. Ananda, and H. S. Lalithamba. (2022): "Green synthesis of tin oxide based nanoparticles using Terminalia bellirica seed extract: impact of operating temperature and antimony dopant on sensitivity for carbon dioxide gas sensing application." *Materials Technology*, pp. 1-8.
19. M. Liu Xuyan, Jiahuan Zeng, Huinan Yang, Kai Zhou, and Deng Pan. (2018): "V₂O₅-based nanomaterials: synthesis and their applications." *RSC advances*, 8, no. 8, pp. 4014-4031.
20. Latif, Muhammad Moazzam, Faheem Amin, Muhammad Ajaz-un-Nabi, Ikram-ullha Khan, and Nadeem Sabir. (2021): "Synthesis and antimicrobial activities of manganese (Mn) and iron (Fe) Co-Doped cerium dioxide (CeO₂) Nanoparticles." *Physica B: Condensed Matter*, 600, p. 412562.
21. Ali, Attarad, Muhammad Zia Hira Zafar, Ihsan ul Haq, Abdul Rehman Phull, Joham Sarfraz Ali, and Altaf Hussain. (2016): "Synthesis, characterization, applications, and challenges of iron oxide nanoparticles." *Nanotechnology, science and applications*, 9, no. 49.
22. Leal L. R. F, Y. Guerra, E. Padrón- Hernández, A. R. Rodrigues, F. E. P. Santos, and R. Peña-Garcia. (2019): "Structural and magnetic properties of yttrium iron garnet nanoparticles doped with copper obtained by sol gel method." *Materials Letters*, 236, pp. 547-549.
23. Y. Veeraswamy, Y. Vijayakumar, and R.R. Reddy. (2014): "Growth and Micro Structural Characterization of In₂O₃ Thin Films Prepared by Electron Beam Evaporation Technique." *Journal of Research in Engineering and Technology*, 5, pp. 267-272.
24. Praveenkumar K, T. Sankarappa, J. S. Ashwajeet, and R. Ramanna. (2015): "Dielectric and AC conductivity studies in PPy-Ag nanocomposites." *Journal of Polymers*.